Performance Evaluation of a Finned Solar Air Collector: Numerical and Experimental Investigation

.

ABSTRACT

The present study aimed to highlight the performance evaluation of a finned solar air collector. This device works in forced conversion and is destined to dry products. The necessity of improving the thermal performances of the solar air collector for specific needs has encouraged us to realize this study. For that, we design a model of solar air collector in which, fins are fixed on its absorber to produce a turbulent flow of air. The air gets through the fins in the same row and induces a good distribution, then reduces the dead areas. The determination of temporal the variations of the glass temperature, the ambient surface, the entrance and exist of the collector, the global radiation in addition, constitute the focal point of this study. The results give a maximum temperature of 74.2° C, the exist of the collector, 78.5 ° C at the surface of the glass, and 107.4 ° C at the surface of the absorber able of satisfying the drying process Our prototype because of the particularity of its absorber permits to reach efficiency superior to 45%.

Keywords: *High-pass solar air collector, Heat transfer, experimentation, efficiency, simulation*

1. INTRODUCTION

Air collectors can be used in many applications requiring low and moderate temperatures, such as space heating, drying agricultural products, drying wood, drying bricks, and so on. Most research is devoted to the development of solar water heaters from the point of view of thermal efficiency in general, but very few studies have been carried out on solar collectors using air as a heat transfer fluid, since the latter has a much lower coefficient of heat transfer by conduction-convection between the absorber and the fluid, compared with that of water. The efficiency of a solar collector, designed to convert solar energy into thermal energy, depends on its shape, the technology chosen and the way in which heat losses at the collector's surface are reduced. So, to improve the performance of these collectors, it is essential to help improve the contact surface between the air and the absorber. Increasing the collector surface area increases the rate of solar radiation intercepted and the contact surface between the absorber and the heat transfer fluid (air) (increasing the exchange surface area), but also increases the heat loss coefficient between the cover and the outside [14-16]. However, the elongation of the solar collector has a strong influence on its efficiency (Karsali; 2007). For this reason, researchers have proposed increasing the heat transfer coefficient between the absorber and the heat transfer fluid without affecting the dimensions of the collector by adding obstacles or fins attached to the underside of the absorber (Abene et al;2004). According to these authors, obstacles can increase the exchange surface, reduce dead zones and create turbulence. This in turn will increase the overall exchange coefficient between the heat transfer fluid and the absorber and promote heat transfer between the two. In the same vein, Abene et al (2004) have shown that the shape, dimensions, orientation and layout of these obstacles have a considerable influence on the efficiency of the collector (as highlighted by Ahrwal and Gandhi (2008)).

Materials and method

The development of solar collector technology therefore requires optimisation of the process at all levels. Thus, the main objective of this study is to improve the performance of the air collector, through the addition of another form of fin.

2. Operating principle of the high-pass finned air collector

2.1 Description of the collector

Our work involves studying the performance of a high-pass finned solar air collector for a hybrid dryer at the Laboratory of Environmental Physics and Chemistry (LPCE), designed for drying food products. This type of dryer uses solar energy combined with another form of additional energy, biomass. This additional source of energy is an alternative means of drying food during periods of low sunlight or at night [17,18]. From an architectural point of view, the dryer consists of a flat solar collector, a drying cage, an extractor powered by a photovoltaic system to automate the system's operation, and a device for using butane gas fitted with a burner. Our work consists solely of studying the performance of the solar collector in this system.

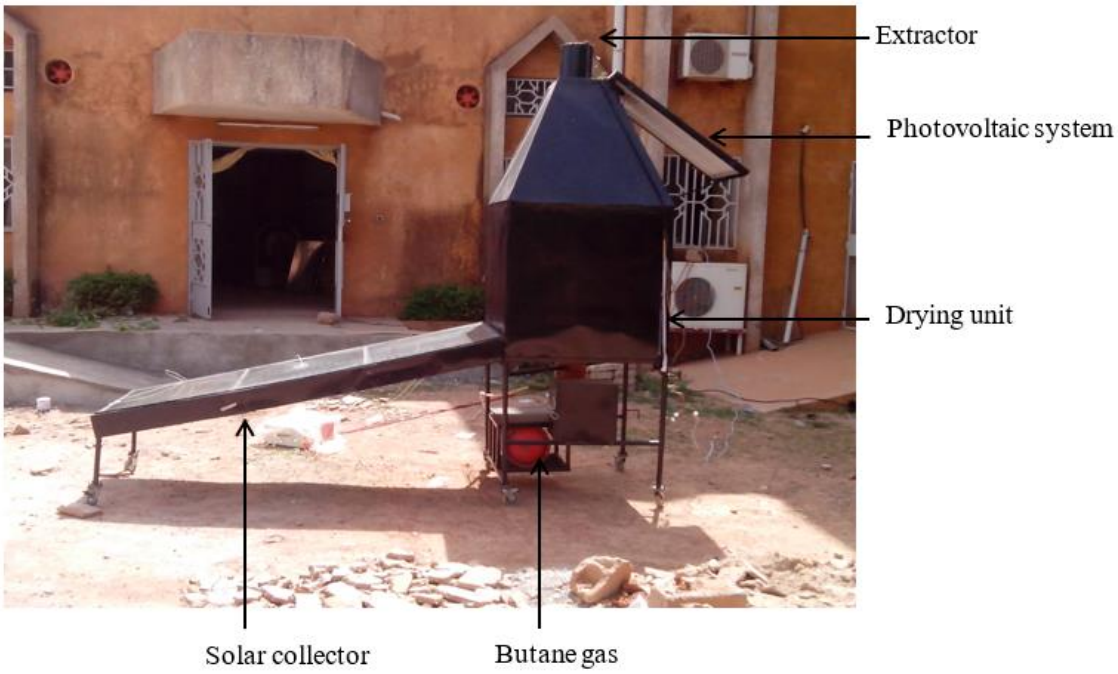

Fig.1. Photo of the dryer

The solar thermal collector shown above (fig.2) consists mainly of a transparent cover (glass), an absorber, a pipe to allow air to collect the energy released by the absorber, and insulation. The special feature of this collector is that fins have been welded on to the absorber to increase the surface area exchanged with the air.

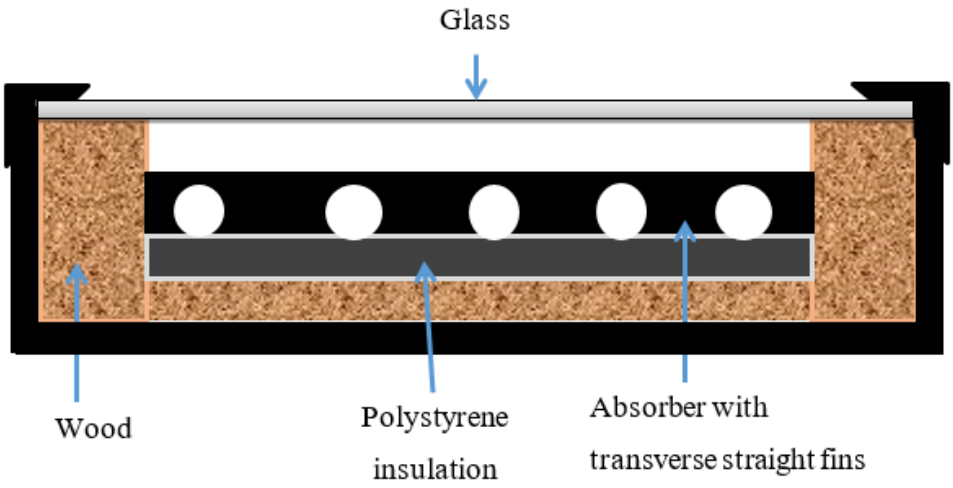

Fig.2. Cross-section of collector

2.2. Thermophysical and geometrical characteristics

2.2.1. Thermo-physical characteristics

The thermo-physical characteristics of the materials used in the design are illustrated in the table 1 below.

Table. 1: Thermo-physical characteristics [3]

Design elements	**Materials**	**Volumic mass** Kg/m^3	**Specific heat** J/kg.K	**Thermal conductivity** $W/m\circ K$
Cover	glass	2700	840	0.93
Absorber	Steel	$7.85.10^{-3}$	500	50.2
Insulation	Polystyrene	20	500	0.04
Box	wood	535	272	0.059

2.2.2. Geometric characteristics.

As for the geometric characteristics, Table 2 shows the different dimensions used in the design of our system.

Table. 2: Geometric characteristics

Design elements	**Length (m)**	**Width (m)**	**Thickness (mm)**
Cover	2.02	0.93	5
Absorber	2.4	0.9	0.27

Fin	0.86	0.05	0.27
Box	2.1	1	50

2.3 Operating principle

The principle of operation of this collector is as follows: solar radiation falling on the surface of the collector passes through the transparent cover (consisting in this case of a pane of glass) and reaches the finned absorber. The absorber absorbs it, heats up and transmits some of the thermal energy to the circulating air, and re-emits long-wave thermal radiation to the outside.

2.4 Fin function

The role of the fins is to increase the convective exchange surface with the air passing through the absorber in order to facilitate heat transfer. The shape and arrangement of the fins also affect the flow of air as it passes through the collector. They ensure good irrigation of the absorber, create turbulence and reduce inactive zones in the absorber. They also improve the heat exchange coefficient.

3. Mathematical formulation

3.1 Simplifying assumptions

Certain assumptions are necessary for an approximate simulation of the system. Thus, in the present study, we assume that:

- The properties of the materials are considered constant;
- The temperature of the ground is taken to be equal to the ambient temperature;
- The sun is considered to be a black body;
- Radiant heat exchange surfaces are assumed to be grey and diffuse;
- Heat flows are one-dimensional;
- The wind direction is parallel to the glass surface;

3.2 Heat transfer modes in the collector

The figure below illustrates the various heat exchanges taking place at the level of a mesh in the collector, and the equivalent diagram for a mesh in the collector is shown:

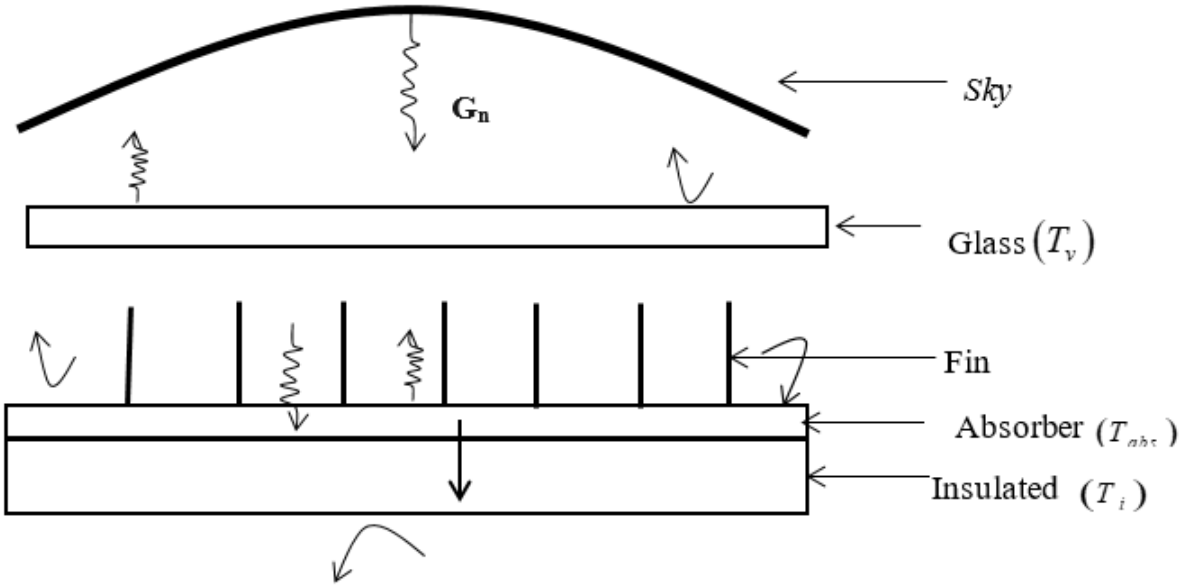

Fig.3. Longitudinal section of the solar collector

3.3 Collector modeling

3.3.1. Energy balance

- *Energy balance* on the cover

$$m_v C_{pv} \frac{dT_v}{dt} = \alpha_v G_n S_v + h_{cv-f-v} S_v (T_f - T_v) + h_{r-abs-v} S_t (T_{abs} - T_v) - h_{cv-v-ext} S_v (T_v - T_{am}) - h_{r-v-c} S_v (T_v - T_c) \quad (1)$$

With : $S_t = \eta_{ai} . \eta_{ai} . S_{ai} + S_{abs}$: total surface exchanged ; (2)

η_{ai} : number of fins on the absorber; S_{ai} : exchange surface of a fin; S_{abs} : absorber surface ; η_a fin efficiency

- ***Energy balance of absorber plate***

$$m_{abs} C_{p_{abs}} \frac{dT_{abs}}{dt} = G_n (\tau\alpha)_{eff} S_t - h_{cd-abs-is} S_{abs} (T_{abs} - T_{is}) - h_{r-abs-v} S_t (T_{abs} - T_v) - h_{cv-abs-f} S_t (T_{abs} - T_f) \quad (3)$$

- ***Energy balance one the airstream***

$$\dot{m}_f C_{pf} \frac{dT_f}{dx} = h_{cv-abs-f} \left(n_{ai} \eta_{ai} l_{ai} + \frac{S_{abs}}{l_{abs}} \right) (T_{abs} - T_f) - l h_{cv-f-v} (T_f - T_v) \quad (4)$$

l_{ai} : fin width ; l : solar collector width ; l_{abs} : width of remaining absorber surface.

- ***Energy balance on the internal wall of bottom insulation***

$$m_{is}C_{pis}\frac{dT_{is}}{dt}=-h_{cv-is-ext}.s_{is}(T_{is}-T_{am})+h_{cd-abs-is}.s_{abs}(T_{abs}-T_{is}) \quad (5)$$

3.3.2 Determination of heat transfer coefficients

- **The convective transfer coefficient between the glass and the ambient air**

The convective exchange coefficient between the collector glass and the ambient air depends mainly on the wind speed and can be evaluated using the Hottel and Woertz relation

$$h_{cv-v-ext}=5.67+3.86V \quad (6)$$

Where V is the wind speed expressed in m/s. This speed must be less than 5m/s.

- **The convective transfer coefficient between the absorbing plate and the glass**

The convective exchange coefficient between the confined air, the glass and the absorbing plate can be written as follows (Jannot, 2007):

$$h_{cv-p-v}=\frac{Nu.\lambda_{air}}{l} \quad (7)$$

Where:

$$Nu=1+1,44\left[1-\frac{1708(\sin 1,8\theta)^{1,6}}{Ra.\cos\theta}\right]\left[1-\frac{1708}{Ra.\cos\theta}\right]^{*}+\left[\left(\frac{Ra.\cos\theta}{5830}\right)^{1/3}-1\right]^{*}$$

$$Ra=\frac{g.\beta.\Delta T.l^{3}.\Pr}{\upsilon^{2}}; \quad 0°\le\theta\le 70° \quad (8)$$

Where expressions followed by an asterisk $[\ ]^{*}$ are taken as zero if their value is negative. R_a is the Rayleigh number, θ the inclination of the collector-adsorber (°), g=9.81 m/s² the gravitational constant, l the characteristic length; $\Pr$ and υ respectively the Prandtl number and the kinematic viscosity of air.

- **The radiative transfer coefficient between the glass and the absorber plate**

The radiative transfer coefficient between the glass and the absorber plate is given by (Duffie and Beckaman, 1974):

$$h_{r-p-v} = \frac{\sigma}{\frac{1}{\varepsilon_p} + \frac{1}{\varepsilon_v} - 1}\left(T_p^2 + T_v^2\right)\left(T_p + T_v\right) \quad (9)$$

- **The radiative transfer coefficient between the glass and the sky**

The radiative transfer coefficient between the glass and the sky is determined by the following equation (Duffie and Beckaman, 1974).

$$h_{r-v-ciel} = \sigma \varepsilon_v F_{v-ciel}\left(T_v + T_{ciel}\right)\left(T_v^2 + T_{ciel}^2\right); \quad (10)$$

Where σ, ε_v and F_{v-ciel} are respectively the emissivity

- **The conductive transfer coefficient between the absorber and the insulating base**

The conductive heat transfer coefficient between the absorber and the insulating base of the solar collector is given by the following formula [6]

$$h_{cd-abs-is} = \frac{1}{\left(\frac{E_{abs}}{S_{absis}.\lambda_{is}}\right) + \left(\frac{E_{is}}{S_{absis}.\lambda_{ab}}\right) + \left(\frac{E_{abs}}{S_{absisl}.\lambda_{isl}}\right) + \left(\frac{E_{isl}}{S_{absisl}.\lambda_{ab}}\right)} \quad (11)$$

3.3.3. Global energy losses

- **The coefficient of heat loss to the front of the collector**

The overall heat loss coefficient towards the front of the collector is given by the following relationship :

$$U_{av} = \frac{1}{R_1 + R_2} = \frac{1}{\left(\frac{1}{h_{r-v-c} + h_{cv-v-ext}}\right) + \left(\frac{1}{h_{cv-abs-f} + h_{r-abs-v}}\right)} \quad (12)$$

- **The Coefficient of heat loss to the rear of the collector**

This coefficient is less important than the one above, as the collector is very well insulated at the back. The expression for this coefficient is given by :

$$U_{arr} = \frac{K_{is}}{E_{is}} = \frac{1}{R_3} \quad (13)$$

- **The coefficient of lateral heat loss**

The value of this coefficient is lower than that of the rear loss coefficient, as the lateral surface of the collector is not very large.

$$U_{lat} = \left(\frac{K_{is}}{E_{is}}\right).\left(\frac{A_{lat}}{A_t}\right) \tag{14}$$

The overall external heat loss coefficient is the sum of the three coefficients.

$$U_L = U_{av} + U_{arr} + U_{lat} \tag{15}$$

3.4. Useful power and solar collector efficiency

3.4.1. Useful power

The useful power provided by the air leaving the collector is written as :

$$Q_u = S_t\left[\left(\alpha\tau\right)_{eff} G_h - U_L\left(T_{abs} - T_{am}\right)\right] \tag{16}$$

If the transfer were ideal, we'd have: $T_{fm} = T_{abs}$ and we could write:

$$Q_u = S_t\left[\left(\alpha\tau\right)_{eff} G_h - U_L\left(T_{fm} - T_{am}\right)\right] \tag{17}$$

In fact the condition $T_{fm} = T_{abs}$ is never satisfied. We therefore need to define a local air-absorber transfer efficiency coefficient F'

$$F' = \frac{\left(\alpha\tau\right)_{eff} - U_L\left(T_{abs} - T_{am}\right)}{\left(\alpha\tau\right)_{eff} - U_L\left(T_{fm} - T_{am}\right)} \tag{18}$$

Let :

$$Q_u = F'\left[\left(\alpha\tau\right)_{eff} G_h - U_L\left(T_{fm} - T_{am}\right)\right]S_t \tag{19}$$

Where T_{fm} is the average fluid temperature.
It is convenient to express this useful power in terms of input conditions by defining another overall air-absorber transfer coefficient as :

$$F_R = \frac{\left(\alpha\tau\right)_{eff} - U_L\left(T_{abs} - T_{am}\right)}{\left(\alpha\tau\right)_{eff} - U_L\left(T_{fe} - T_{am}\right)} \tag{20}$$

Where

$$Q_u = F_R\left[\left(\alpha\tau\right)_{eff} G_h - U_L\left(T_{fe} - T_{am}\right)\right]S_t \tag{21}$$

3.4.2. Solar collector efficiency

The overall efficiency of the collector is defined as the quotient of the useful power over the incident power.

$$\eta = \frac{Q_u}{S_t G_n} \tag{22}$$

So equations (21) and (22) give :

$$\eta = F_R \left[(\alpha\tau)_{eff} - U_L \frac{(T_{fe} - T_{am})}{G_n} \right] \tag{23}$$

According to Duffie and Beckaman (1975), the efficiency can be written as :

$$\eta = B + K.T^* \tag{24}$$

with :

$B = F_R(\alpha\tau)_{eff}$: the optical factor of the sensor or an indication of the rate of energy absorption;

$K = F_R.U_L$: the total thermal conductance of the losses or an indication of the rate of energy loss;

$$T^* = \frac{(Tfe - Tam)}{Gn} \tag{25}$$

When the collector is assumed to be in steady state, with the transparent cover and absorber isothermal, the optical factor B and thermal conductance K are constant. The instantaneous efficiency line is found. In reality, B and K vary with the collector's operating temperature and climatic conditions, and are independent of the collector's surface area. $B = F_R(\alpha\tau)_{eff}$ and $K = F_R.U_L$ are the two main parameters that make up the collector model.

3.5. Mathematical resolution

3.5.1. Model of discretization of the equations

The equations (1-5) have been discretized using an implicit finite difference method. This method, based on the Taylor series development, allows to transform the differential equations into a system of linear equations. The resolution of this system of equations requires an iterative calculation to determine the physical quantities as a function of the unknown variables at a given time on the one hand, and the variables known at the previous time t on the other hand. The system of equations thus obtained can be presented as a matrix equation with coefficient [A], variable [T] and second member [B].

3.5.2. Numerical solution procedure

The method of solving the system of equations that describes the transient behavior of the model is purely numerical, based on the implicit finite difference method and the iterative method of Gauss Seidel. A computer program written in Matlab language has been developed to model and simulate, the operation of each element of the solar collector during one day.

4. Experimental environment

4.1 Presentation of the collector

The solar collector studied is a flat-plate air collector with a finned absorber. It comprises:

- A casing made of sheet steel, measuring 2.41 x 1 m, open on the side exposed to solar radiation, with openings for air intake and outlet;
- A pane of glass covering the casing to create a "greenhouse effect";
- An absorber plate to which fins are welded to facilitate heat transfer to the heat transfer fluid (air);
- 5 cm of glass wool insulation at the bottom of the casing, to limit heat loss to the outside.

4.2 Measurement and data acquisition system

The various sensor tests took place at the University of Ouagadougou (Burkina Faso), more specifically at the LPCE laboratory located between latitudes 12°20 and 12°26 North and between longitudes 1°28 and 1°36 West. In this landscape, for the period of the experiments :

- the average monthly ambient temperature varies between 25°C and 34°C,
- average monthly air humidity varies between 24% and 77%,
- average monthly sunshine varies from 1567 J/cm² to 1900 J/cm² [8].

4.2.1. Measurement of solar radiation

Overall solar radiation on the surface of the collector is measured using a KIMO solarimeter. Measurements are taken at fifteen (15) minute intervals.

4.2.2. Temperature measurements

The temperature measurement campaign was carried out in order to be able to estimate the efficiency of the sensor. On each occasion, the data was taken between 8 a.m. and 5 p.m. at fifteen (15) minute intervals. To do this, five (05) type K thermocouples (chromel/alume) were placed on the various components of the solar collector. All the thermocouples are connected to a Testo temperature recorder, which in turn is connected to a computer to acquire the measurement data.

4.2.3. Data acquisition and processing system

The central measuring unit is used for data acquisition. It is controlled by a microcomputer equipped with "Testo-Comfort Software Basic 5" software, which is used to acquire the data. To limit the size of the storage files, we chose measurement intervals of fifteen (15) minutes. The data is processed using Excel software to plot the curves.

5. Results and discussion

5.1 Evolution of solar radiation

Figure 4 shows the comparative evolution of experimental and theoretical global solar radiation as a function of time. It can be seen that the curves increase until they reach a maximum value at around 12h, then gradually decrease with solar activity. The theoretical curve shows a similar trend, with a maximum value of around 980 W/m². Analysis of these

curves reveals a significant difference. This difference is essentially due to cloud disturbance and the environment of the experimental site.

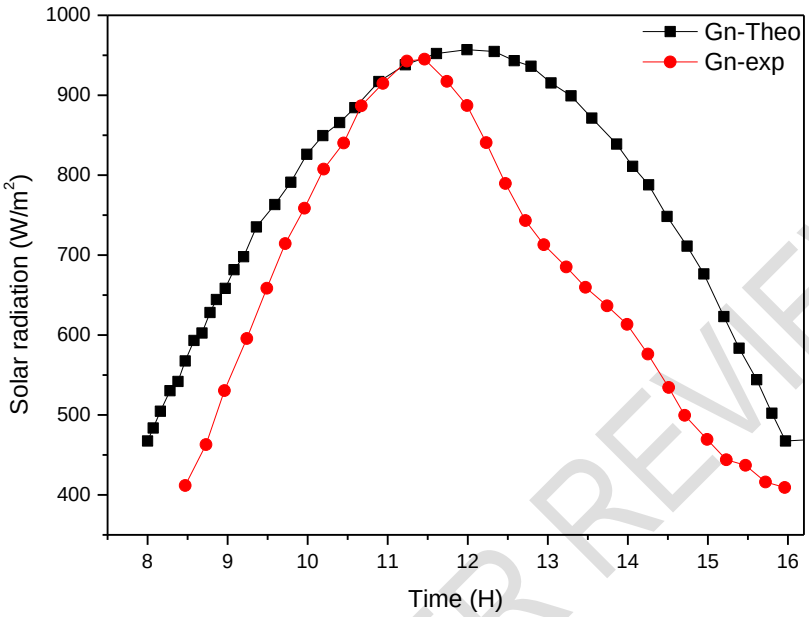

Fig.4. Comparison of theoretical and experimental radiation curves

5.2 Temperature changes in the various elements of the collector

The comparative evolution of the theoretical and experimental temperatures of the various components of the solar collector, i.e. the pane, the absorber and the air at the collector inlet and outlet, are shown in Figure 5. Initially, it can be seen that the temperature of the air at the collector outlet increases less quickly than that of the pane. As the transfers take place, the energy accumulated in the pane and that accumulated by the absorber are transferred to the air, which then gradually increases in temperature. Given the glass pane's low absorption coefficient ($\alpha = 0.14$), its temperature changes little as the day progresses, compared with that of the solar absorber, which reaches higher temperatures of up to 110°C, given its greater absorption capacity ($\alpha = 0.95$). It is therefore important to note that the variation in overall temperatures is particularly dependent on the incident solar power and the surrounding climatic conditions. The results of the theoretical and experimental temperatures of the various elements of the collector as a function of time show a similar pattern. However, the theoretical temperature values are higher than the experimental values. This is due to the presence of clouds, low levels of sunlight and thermal heat loss.

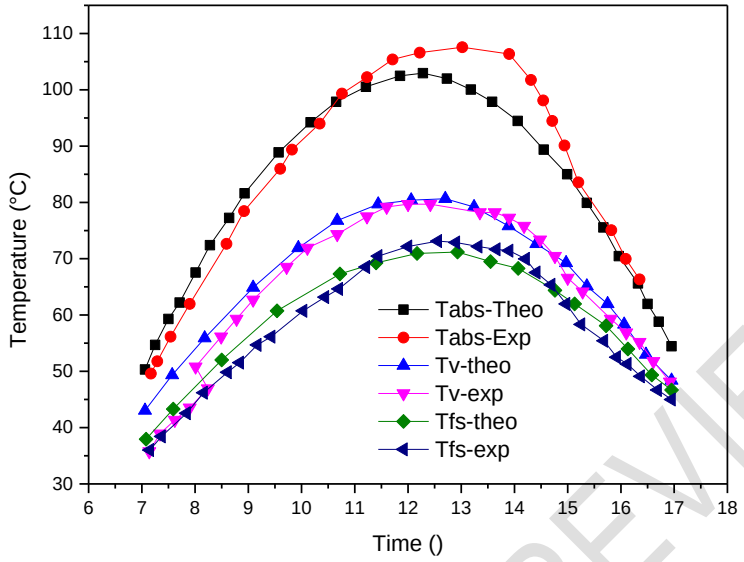

Fig.5. Comparison of theoretical and experimental temperatures

5.3. Collector performance

Figure 6 illustrates the trend in theoretical and experimental performance over the course of a day's experiment. If we compare these curves, we can see that the variations are different. This can be explained by the fact that heat transfer losses are very high and vary from day to day. These heat losses also increase with the rise in air temperature at the collector inlet and outlet respectively. Despite the presence of clouds and low sunshine, the average experimental yield (45%) is higher than the average theoretical yield (39%). This is due to the theoretical approach and the simplifying assumptions imposed at the outset in the theoretical model in order to obtain an approximate simulation of the system. Nevertheless, comparing the collector efficiency obtained (45%) with that of Kabre and Sawadogo (2010) for a flat absorber collector [7], which is 25%, with that of Dissa (2009) for a mixed absorber collector (corrugated sheet metal, porous absorber), which is 36% [8], and that of Housseyn (2011) for an absorber with triangular fins, which is 40% [9], we can conclude that increasing the exchange surface between the air and the absorber by adding fins on the inner surface of the absorber improves the efficiency of air collectors.

Table 3: Comparison of performance

	Flat absorber collector Dissa (2009)	Mixed absorber (corrugated sheet, porous absorber) Kabre and Sawadogo (2010)	Absorber with triangular fins Housseyn (2011)	Present study

Efficiency (%)	25	36	40	45

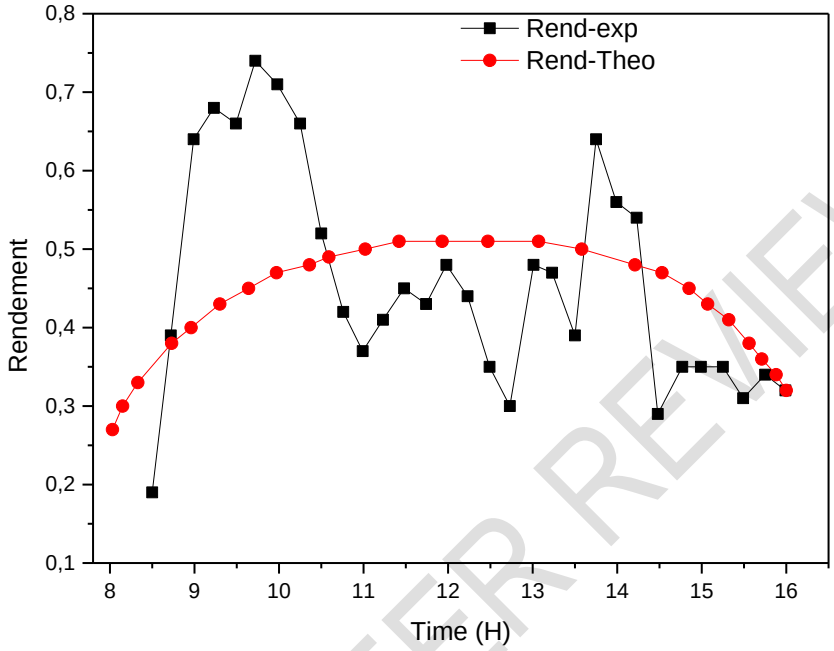

Fig.6. Comparison of theoretical and experimental performance

Conclusion

As part of our work, we were particularly interested in assessing the performance of the finned high-pass air collector. All the results have made it possible to determine the influence of a number of parameters on the operation of the sensor. All the results have made it possible to determine the influence of numerous parameters on the operation of the sensor. This study also enabled us to determine the collector's instantaneous and daily yields under quasi-steady-state conditions. However, the transient regime needs to be taken into account for a more rigorous study. Nevertheless, by comparing the efficiency of our collector (45%) with that of Kabre and Sawadogo (2010) for a flat absorber collector [7], which is 25%, with that of Dissa (2009) for a mixed absorber collector (corrugated sheet metal, porous absorber), which is 36% [8], and that of Housseyn (2011) for an absorber fitted with triangular fins, which is 40% [9], we can conclude that increasing the heat exchange surface by adding fins to the absorber has played a very favourable role in optimising the efficiency of our air collector.

Nomenclature

Cp	Spécific heat (J/kg.K)		Subscripts
Gn	Solar radiation (W/m^2)	**is**	Insulation
m	Mass (kg)	**abs**	absorber
h_{cv-}	Convective transfer coefficient (W/m^{2}K)	**fs**	Outlet fluid

h_r	Radiative transfer coefficient (W/m^{2}K)	**fe**	Inlet fluide
h_{cd}	Conductive transfer coefficient (W/m^{2}K)	**v**	glass
T	Température (K, °C)	**ar**	rear
Q_u	Useful power (W)	**av**	front
S	Area (m^2)	**ext**	outside
U	Loss coefficient (W/m^{2}K)	**amb**	ambient
Nu	Number of Nusselt	**r**	radiative
Gr	Number of Grashoff	**cd**	conductive
Ra	Number of Rayleigh	**cv**	convective
Re	Number of Reynolds	**fm**	Medium fluid
Pr	Number of Prandtl	**ai**	Fin

Disclaimer (Artificial intelligence)

Option 1:

Author(s) hereby declare that NO generative AI technologies such as Large Language Models (ChatGPT, COPILOT, etc.) and text-to-image generators have been used during the writing or editing of this manuscript.

Option 2:

Author(s) hereby declare that generative AI technologies such as Large Language Models, etc. have been used during the writing or editing of manuscripts. This explanation will include the name, version, model, and source of the generative AI technology and as well as all input prompts provided to the generative AI technology

Details of the AI usage are given below:

1.

2.

3.

References

[1] A. BENALLOU, J. BOUGARD, the thermal sun at the service of sustainable development, guide to solar energy, International Solar Energy Network (IESN). IEPF, Canada, Etude et Filière collection; 1986.

[2] D. Semmar, S. Betrouni and D. Lafri, Study and realization of a solar air collector, Rev. Energ. Ren.: Energy Physics (1998) 33 - 38

[3] S. Oudjedi1, A. Boubghal1, W. Braham Chaouch1, T. Chergui1 and A. Belhamri2 Theoretical and experimental study of a solar air collector intended for drying (Part:1) Renewable Energy Review SMSTS'08 Algiers (2008) 237 – 248

[4]. Bouhediba Malika, Thermal simulation of a solar house for the production of domestic hot water (DHW); Hassiba Benbouali University of Chlef Faculty of Technology Department of Mechanical Engineering; 2011.
[5] A. Ahmed-Zaïd 1, A. Moulla 1, M. S. Hantala 1 and J.Y. Desmons, 'Improving the performance of flat air solar collectors: Application to the drying of yellow onion and herring' Rev. Energ. Ren. Vol.4 (2001) 69-78
[6] J. A. DUFFIE, W. A. BECKAMAN, solar energy thermal process. A wiley-instersciences publication 1974
[7] S. Kabre, M. Sawadogo, Study of the performance of a flat solar collector field, Renewable Thermal Energy Laboratory (L.E.T.RE) University of Ouagadougou, 2010
[8]. A.O. Dissa, J. Bathiebo, S. Kam, P.W. Savadogo, H. Desmorieux, J. Koulidiati; Modeling and experimental validation of thin layer indirect solar drying of mango slices; Laboratory of Environmental Physics and Chemistry (LPCE), Training and Research Unit in Exact and Applied Sciences (UFR/SEA), University of Ouagadougou
[9] T. Koyuncu, Performance of various designs of solar air heaters for crop drying applications, Renewable Energy 31 (2006) 1073–1088.
[10] Roger Bernard, Gilbert Menguy, Marcel Schwartz; Solar radiation thermal conversion and applications. 2nd edition TECHNIQUE AND DOCUMENTATION
[11] Daguenet Michel (1985). Solar Dryers: Theory and Practice, UNESCO, France.
[12] Abene, A., Dubois, V., Le Ray, M., Ouagued, A., 2004. Study of a solar air flat plate collector: use of obstacles and application for the drying of grape. J. Food Eng. 65, 15–22. doi:10.1016/j.jfoodeng.2003.11.002
[13] Karsli, S., 2007. Performance analysis of new-design solar air collectors for drying applications. Renew. Energy 32, 1645–1660. doi:10.1016/j.renene.2006.08.005
14. Aissaoui, F., Benmachiche, A. H., Brima, A., Bahloul, D., & Belloufi, Y. (2016). Experimental and theoretical analysis on thermal performance of the flat plate solar air collector. International Journal of Heat and Technology, 34(2), 213-220.
15. Aissaoui, F., Benmachiche, A. H., Brima, A., Belloufi, Y., & Belkhiri, M. (2017). Numerical study on thermal performance of a solar air collector with fins and baffles attached over the absorber plate. International Journal of Heat and Technology, 35(2), 289-296.
16. Belloufi, Y., Rouag, A., Aissaoui, F., Benmachiche, A. H., & Brima, A. (2023). Thermal Performance of Double Pass Solar Air Collector: Numerical and Experimental Investigation. Annals of West University of Timisoara-Physics, 65(1), 124-143.
17. Ky, Thierry S. M., Salifou Ouedraogo, Moctar Ousmane, Boureima Dianda, Emmanuel Ouedraogo, and Dieudonné J. Bathiebo. 2021. "Experimental Study of a Stationary Hot Air Solar Collector Built With Hemispherical Concentrators and Enhanced With Fresnel Lenses". Physical Science International Journal 25 (1):8-22. https://doi.org/10.9734/psij/2021/v25i130233.
18. Ouedraogo, Boukaré, Boureima Dianda, Kalifa Palm, and Dieudonné Joseph Bahiebo. 2015. "Influence of Adding Rectangular Fins on the Performances of a Thermal Solar Air Plane Collector". Current Journal of Applied Science and Technology 11 (6):1-11. https://doi.org/10.9734/BJAST/2015/20741.